

***Ab initio* calculation of Peierls stress in silicon**

Masayasu Miyata and Takeo Fujiwara

*Department of Applied Physics, University of Tokyo, Bunkyo-ku, Tokyo 113-8656, Japan*

(Received 31 March 2000; revised manuscript received 23 August 2000; published 9 January 2001)

The Peierls stress of a straight screw dislocation in Si has been studied by an *ab initio* molecular dynamics simulation. The generalized stacking fault energy in Si can no longer be the continuous function of displacement of the slip plane with structural relaxation. Then the Peierls-Nabarro theory fails to describe properties of the dislocation core, such as the Peierls stress. Direct simulation of the slip dynamics of dislocations has also been performed and the Peierls stress is derived without any artificial modeling of a dislocation core with an excellent agreement with experimental results. The effect of the Peierls potential on the slip dynamics of dislocations is also discussed.

DOI: 10.1103/PhysRevB.63.045206

PACS number(s): 61.72.Lk, 62.20.Fe

**I. INTRODUCTION**

The plastic deformation of crystals is governed by the dynamics of dislocations. A dislocation is a physical entity of the continuum theory of elasticity. It moves in an intrinsic periodic potential field of the lattice, called the Peierls potential, driven by an external stress. Though realistic situations are naturally more complicated, basic physical properties of dislocations should be studied in the simplest situation of an isolated straight dislocation at 0 K.

In order to realize this situation in experiments, deformation tests of materials have been done with keeping the dislocation density as low as possible at very low temperatures. Silicon is an ideal material to have a single crystal with low dislocation density. However, in order to investigate the plasticity of Si, we could encounter several difficulties as follows. First, it is difficult to deform semiconductor crystals at lower temperatures without brittle fracture. Recently, deformation tests of semiconductor crystals have been conducted under confining hydrostatic pressure to avoid brittle fracture,<sup>1,2</sup> and their yield stress shows strong temperature dependence.<sup>3,4</sup> With decreasing temperatures, the yield stress of Si increases up to a value higher than 1 GPa at about 600 K.<sup>5</sup> Then, one could not extrapolate the value of the yield stress to 0 K in order to estimate the value of the Peierls stress. Furthermore, in this experimental procedure, the effect of the high confining hydrostatic pressure on the dislocation properties is still unknown. Second, the conventional dislocation model of an elastic string does not work, because of the sharpness of the dislocation kink in a material of high Peierls potential. The Peierls potential in Si is very high because of its covalency and higher brittleness. Therefore, it is important to study several properties of dislocations in Si from the atomistic calculation.

Among atomistic calculations, the *ab initio* molecular dynamics (AIMD) simulation is the most desirable way to get information of covalent systems because the change of electronic structure is essential to determine their mechanical properties. There have been many efforts to connect the discrete atomistic information with the linear continuum description and then know the plastic properties. One of the useful approaches was proposed and developed by Vitek and co-workers.<sup>6,7</sup> They introduced a new physical quantity,

called the generalized stacking fault (GSF) energy. Once one gets the GSF energy, then one calculates various plastic properties by way of the Peierls-Nabarro (PN) theory. The GSF energy of Si was first calculated by Kaxiras and Duesbery with AIMD.<sup>8</sup>

An alternative approach is the direct simulation of dislocation slip, where a dislocation is forced to move by an applied external force. The atomic structure of dislocation core of a screw dislocation in Si was given by Hornstra.<sup>9</sup> Arias and Joannopoulos showed the stability of that structure by AIMD.<sup>10</sup>

In the present paper, we performed two kinds of AIMD simulation of slip dynamics of dislocations. The first is the shearing process of a perfect Si crystal at the (111) slip plane, followed by structural relaxation. This process provides a profile of the GSF energy as a function of the displacement on the slip plane. The second is the deformation process of a crystal with straight dislocations, accompanied by the structural relaxation. This process provides a slip dynamics of straight dislocations in accordance with the increase of the external stress field. The outline of the present paper is as follows. In Sec. II, we review the known slip system and dislocations in Si. In Sec. III, we will explain the simulation methods for the dislocation properties. Section IV is devoted to present our results and discussions. We give our conclusions in Sec. V.

**II. SLIP SYSTEM OF DISLOCATIONS IN SILICON**

The natural cleavage planes and slip directions in diamond structure are  $\{111\}$  planes and  $\langle 110 \rangle$  directions. There are two kinds of perfect dislocations in diamond structure, a screw and a  $60^\circ$  dislocation, where the latter term arises from the  $60^\circ$  angle between the direction of the dislocation line and the Burgers vector. These dislocations are dissociated into Shockley partial dislocations at high temperatures. A screw dislocation dissociates into two  $30^\circ$  partial dislocations, and as does a  $60^\circ$  dislocation into a  $30^\circ$  and a  $90^\circ$  partial dislocation.

According to the two kinds of different intervals between  $\{111\}$  planes, there are two ways of moving dislocations in a  $\{111\}$   $\langle 110 \rangle$  slip system. One way is that the slip motion occurs between two planes of the interval equal to the bond

length, and this is called a *shuffle* set. The other way is that slip motion occurs between two planes of the interval equal to  $1/3$  of the bond length, which is called a *glide* set. There has been a controversy about the most probable case for moving dislocations.<sup>11</sup> One may predict that the shuffle set is selected, because, in the slip process, one bond per atom should be rearranged for the shuffle set while three bonds per atom are rearranged for the glide set.

The partial dislocations are experimentally observed to move in the glide set with being bound by the stacking fault. On the shuffle set, partial dislocations do not move without diffusive dragging of a row of vacancies. Therefore, one expects that the resistance of motion in the shuffle set is higher than that in the glide set. Thus the experimental results are supposed, at least at high temperatures, to support the slip mechanism of the glide set, in contrast to the above intuitive prediction.

On the other hand, a preliminary dynamical AIMD simulation, at low temperatures, of shear deformation of a Si crystal shows that the perfect crystal is broken at the shuffle set.<sup>12</sup> This result is consistent with the above intuitive prediction, and we presume that the shuffle set is selected as the slip system in the detailed simulation study in the present paper.

### III. METHODS TO CALCULATE PEIERLS STRESS

#### A. Technical details of AIMD

The AIMD simulation of Si crystals was done by using the method of direct minimization of the energy functional of the local density approximation<sup>13</sup> (LDA), including partially occupied and unoccupied orbitals together with occupied Kohn-Sham (KS) single-electron orbitals.<sup>14</sup> All atoms, except those on clumped layers in the calculation of the GSF energy, were allowed to move along any direction. We used only the  $\Gamma$  point ( $\vec{k} = \vec{0}$ ) in the Brillouin zone and an energy cutoff, for the plane wave expansion,  $E_{\text{cut}} = 8$  Ry in the calculation of the GSF energy and  $E_{\text{cut}} = 10$  Ry in the deformation dynamics of dislocations. We used the soft norm-conserving pseudopotential by Troullier and Martins<sup>15</sup> with the Kleinman-Bylander separable form.<sup>16</sup> The local exchange correlation functional of Ceperly and Alder parametrized by Perdew and Zunger<sup>17</sup> was used.

#### B. Indirect method: GSF energy and block shearing process

Consider the process in which an infinite crystal is cut into two semi-infinite parts, parallel to an atomic plane. The upper half part of the crystal is shifted parallel to the cut atomic plane with respect to the lower half by a certain displacement vector  $\vec{f}$ . This process is called *block shearing*. The energy increase per unit area on the slip plane associated with the displacement vector is defined as the GSF energy  $\gamma(\vec{f})$ . The differentiation of  $\gamma(\vec{f})$  with respect to  $\vec{f}$ ,  $-\partial\gamma(\vec{f})/\partial\vec{f}$ , is the restoring force due to the misfit between the two parts of the lattice.

To simulate block shearing process for the calculation of the GSF energy, we used a supercell consisting of twelve (111) atomic planes, totally 72 atoms, under the periodic

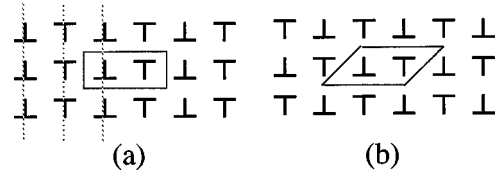


FIG. 1. (a) Dipolar lattice of dislocations and (b) quadrupolar lattice. This figure is the same as Fig. 2 in Ref. 21.

boundary condition. The mirror symmetry was reserved during the shearing process with respect to the central (111) planes. We cut the half semi-infinite block of the crystal on the shuffle set along  $[\bar{1}\bar{1}2]$  direction with two clamped planes farthest from the cut. Then the LDA energy functional was minimized by atomic relaxation along arbitrary directions, until the total force was reduced to be less than 0.005 Ry/(a.u. atom). The accuracy of the total energy is proved to be less than 0.05 Ry/(super cell), and that of the GSF energy is less than 5% throughout the simulation.

We can specify the displacement of two halves of the cut crystal as follows. The vector  $\vec{f}$  is the displacement vector of the two atomic planes immediately adjacent to the cut. The GSF energy of the unrelaxed cut crystal was defined by Vitek.<sup>6</sup> The relative displacement can also be defined in a different way by using the displacement vector  $\vec{f}_C$  between the centers of the two semi-infinite parts of the crystal.<sup>18</sup> Therefore,  $\vec{f} = \vec{f}_C$  in case of unrelaxed system, and  $\vec{f} \neq \vec{f}_C$  in case of relaxed system.

Following Ref. 18, we measured the GSF energy  $\gamma(\vec{f})$  as a function of the displacement vector  $\vec{f}$ . After structural relaxation, the dangling bonds disappear and the system holds rearranged bonds with large distortion. Therefore, the  $\gamma(\vec{f})$  after relaxation is not actually the generalized ‘‘stacking fault’’ energy, but just the energy with distortions, though we would still call it the GSF energy.

#### C. Direct method: Simulation of dislocation motion

##### 1. Configuration of dislocations for simulation

An isolated dislocation is accompanied by a long-range strain field and the resultant strain energy is diverged. Therefore one should introduce a dislocation dipole in the system and then the strain field may damp within a certain finite range. However, under a periodic boundary condition, a dislocation dipole in a rectangular unit cell makes grain boundaries toward the direction normal to the dipole array, as shown in Fig. 1(a).<sup>19</sup> These grain boundaries cause a spurious shear strain and change the electronic state. The better choice may be the quadrupole arrangement of dislocations because the spurious strain is eliminated. Then another difficulty appears if we use a rectangular unit cell, e.g., the quadrupolar configuration makes the system size double in the array of rectangular unit cells. Because a large amount of computational resource is required in AIMD, one should try to keep the system size minimal as much as possible. So we adopt an oblique superlattice that realizes a quadrupolar con-

figuration under periodic boundary conditions and whose unit cell contains one dislocation dipole, as shown in Fig. 1(b).<sup>19</sup>

In an actual simulation, our unit cell of oblique supercell consists of six (111) atomic planes and of two times and five times the primitive cell towards  $a$  and  $b$  directions, respectively, totally 120 Si atoms in an oblique unit cell. The unit cell is shown in Fig. 4. Each direction of the  $a$  and  $b$  axis is  $[\bar{1}10]$  and  $[\bar{1}\bar{1}2]$ , respectively. A dipole of screw dislocations in shuffle set was introduced into the unit cell. The core structure of a dislocation in glide set is not known and considered to be unstable. The core structure of a shuffle screw dislocation was given by Hornstra<sup>9</sup> and proved to be stable by Arias and Joannopoulos<sup>10</sup> by AIMD. The crystal was uniformly deformed towards  $[\bar{1}10]$  direction. Then the LDA energy functional was minimized by atomic relaxation, until the total force was reduced to be less than 0.001 Ry/(a.u. atom). The accuracy of the total energy is proved to be less than  $0.92 \times 10^{-3}$  Ry/(supercell). According to Ref. 10, the spontaneous mutual annihilation of a dislocation dipole occurs when the dislocation contacts another. The supercell used in the present simulation is large enough to avoid this annihilation of dislocations because after the slip motion by one period of the lattice dislocations do not contact yet.

## 2. Superposition assumption of strain field and interaction between dislocations

When the system is large enough, we suppose that the superposition principle does work in the following terms: (1) the strain field by dislocations and that by crystal deformation and (2) the interaction between dislocations. The elastic term involves elastic interactions between dislocations. According to the above superposition assumption, the nonlinear term can be neglected in the nonelastic term. Then the nonelastic energy consists only of the Peierls potential and the energy of deformation of perfect crystal.

## IV. RESULTS OF SIMULATIONS AND DISCUSSIONS

### A. GSF energy by block shearing

The AIMD of the block shearing process was done for displacement vectors  $f_C \equiv |\vec{f}_C| = 0, 0.125b, 0.25b, 0.3125b, 0.375b, 0.4375b, 0.46875b,$  and  $0.5b$ , where  $b$  is the amplitude of the Burgers vector. It should be mentioned here that the change of the amplitudes of  $\vec{f}$  perpendicular to slip direction after relaxation is much smaller than those of  $\vec{f}$  parallel to the slip direction, by a factor of several orders of magnitude, at most by a factor of  $10^{-2}$ . Then we compare the profiles of the GSF energies with and without structural relaxation, only on the same plane parallel to the slip direction.

#### 1. GSF energy

Figure 2 shows the GSF energy profile of the displacement along the  $[\bar{1}\bar{1}2]$  direction obtained by the AIMD simulation. The shape of the GSF energy  $\gamma(\vec{f})$  gets split into two parts after the relaxation, as shown in Fig. 2. The atomic configurations without structural relaxation after block shear-

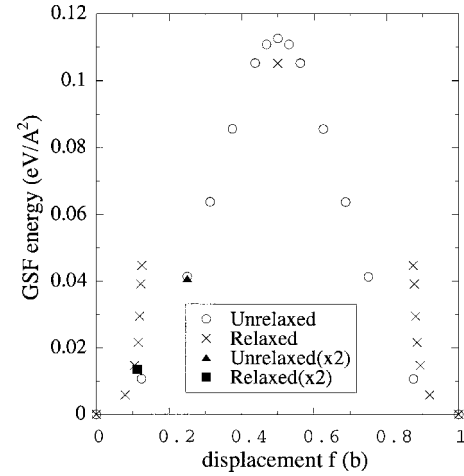


FIG. 2. The GSF energy profile toward  $[\bar{1}\bar{1}2]$  direction on the shuffle set of (111) planes, without (open circles)/ with (crosses) structural relaxation of atomic positions. The results for double size along  $[111]$  direction are also shown for both cases of without (solid triangle) and with (solid square) structural relaxation. Each of the open circle corresponds to each of the cross with the same  $f_C$ .

ing are associated with dangling bonds and are unstable. After structural relaxation, the dangling bonds or the stacking fault disappears and the system has a large distortion. Therefore, the real structure of a dislocation core for covalent systems cannot be the continuous stacking fault, because the bonds are abruptly rearranged.

To see if the shape of  $\gamma(\vec{f})$  with structural relaxation depends on the system size, we doubled the size of the unit cell along the  $[111]$  direction in Si with  $f_C = 0.25b$ . We do not observe any qualitative differences of results, in Fig. 2, between two unit cell sizes and, therefore the present unit cell size is enough large.

The shear modulus  $\mu$  can be estimated from the shape of  $\gamma(\vec{f})$  with a small  $f_C$  as  $\mu = 0.48 \text{ eV}/\text{\AA}^3$ , which agrees well with the experimental value  $\mu = 0.43 \text{ eV}/\text{\AA}^3$ .<sup>20</sup> The characteristic values obtained from the shape of  $\gamma(\vec{f})$  are the peak of the GSF energy  $\gamma_{us}$ , called the *unstable stacking fault energy*,<sup>21</sup> and the maximum of restoring force  $\tau_{\max} \equiv \text{Max}[-\partial\gamma(\vec{f})/\partial\vec{f}]$ . We get  $\gamma_{us} = 0.105 \text{ eV}/\text{\AA}^2$  and  $\tau_{\max} = 0.086 \text{ eV}/\text{\AA}^3$  and the dislocation width  $2\zeta = 0.88b$ . These values are almost the same as those calculated in Ref. 22.

#### 2. Peierls stress from indirect method

The GSF energy without structural relaxation can be represented well by a continuous sinusoidal function for which the PN equation have an analytic solution. The Peierls stress from the PN theory is

$$\sigma_p = 0.032 \text{ eV}/\text{\AA}^3, \quad (1)$$

which is relatively small value compared with those expected from experiments  $\sigma_p = 0.043 - 0.215 \text{ eV}/\text{\AA}^3$ .<sup>23</sup>

We performed a similar simulation of block shearing in GaAs. The results of GaAs are almost the same as those of Si. The Peierls stress of GaAs is nearly the same as the value

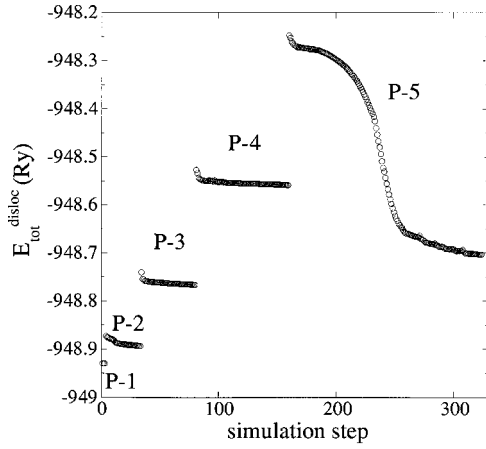


FIG. 3. Change of total energy as a function of simulation step in the deformation process of a crystal with straight dislocations.

in Si estimated by the PN theory, while that is expected to be smaller by one order of magnitude than experimental values in Si. The calculated values by the present indirect simulation are estimated as

$$\sigma_P = 0.026 \text{ eV}/\text{\AA}^3, \quad (2)$$

using experimental value of shear modulus for GaAs  $\mu = 0.31 \text{ eV}/\text{\AA}^3$ .<sup>24</sup> From our simulation,  $\mu$  is obtained as  $\mu = 0.35 \text{ eV}/\text{\AA}^3$ . The values of  $\gamma_{us}$  and  $\tau_{max}$  in GaAs are actually almost equal to those values derived by scaling the values in Si by a factor of the covalency 0.88 in GaAs.<sup>25</sup>

The quantitative disagreement of plastic properties, such as  $\sigma_P$ , may be due to the insufficient treatment of dislocation core structure. This seems to be crucial especially for narrow core systems like semiconductor crystals. One should, therefore, try the direct slip simulation of dislocations.

## B. Slip dynamics of dislocations caused by crystal deformation

### 1. Deformation process

Next we performed AIMD simulation of structural relaxation after the shear deformation of crystal containing straight dislocations. The crystal is uniformly deformed toward the direction parallel to the Burgers vector in accordance with the change of primitive vectors that span the simulation unit cell. Though this process is different from the block shearing, we still use the displacement vector  $\vec{f}_C$  of the same definition to refer the degree of shear deformation. We did the dislocation slip through the processes of crystal deformation and structural relaxation for  $f_C \equiv |\vec{f}_C| = 0, 0.1b, 0.2b, 0.3b$ , and  $0.4b$ . In the following, we call these processes as P-1, P-2, . . . , and P-5, respectively. During process P-5, we observed the slip of screw dislocations. After the process P-5, we unloaded the external stress and relaxed the structure again. This process is referred to as P-6.

Figure 3 shows the change of the total energy as a function of simulation steps. Ions move during each simulation step to minimize the total energy after the uniform shear deformation of the crystal. After structural relaxation, further deformation follows. As the deformation gets larger, so does

the energy increase after the deformation. The reduction of the total energy after structural relaxation is at most 0.04 Ry/cell, except that for the P-5 process. The reduction of the total energy at the beginning of the P-5 process is larger than that of any other process. The dislocations slip in the region of  $0.3b < f_C < 0.4b$  after the dislocations overcome the barrier of the Peierls potential.

### 2. Change of core structures

Figure 4(a) shows the atomic configuration of the oblique unit cell observed after process P-1. The resultant structure preserves the fourfold coordination of each Si atom and is stable. The maximum deviation of the bond length from the average is within 5.5%. Furthermore, we observed that the strain field around the dislocation core of the opposite sign holds the inversion symmetry. Figure 4(b) shows the atomic configuration of the oblique unit cell observed after process P-5. The distance between the dislocations in the dislocation dipole has changed, and a dislocation moves by a translation period of the crystal lattice.

We show in Table I, to ascertain the slip of dislocations, the bond lengths and the bond angles near the dislocation core after each process. During  $f_C < 0.3b$ , the bond length of  $A-B$  decreases and those of  $C-D$  and  $E-F$  increase with increasing crystal deformation  $f_C$ . The positions of atoms denoted by  $A$  to  $F$  and  $X$  to  $Z$  can be seen in Fig. 4. Thus the position of the dislocation core is located between the bonds of  $A-B$  and  $C-D$  and moves gradually toward the  $+b$  direction. Changes of bond angles for each process also show this movement of the dislocation core.

After the process P-5 of  $f_C = 0.4b$ , we observed the abrupt increase of the bond length of  $C-D$  and decrease of that of  $C-D'$ . The  $C-D$  bond length becomes nearly equal to those of  $A-B$  and  $C-D$  at  $f_C = 0$ . Thus the bond switches abruptly from  $C-D$  to  $C-D'$  in the range  $0.3b < f_C < 0.4b$ .

Investigating bond lengths and angles of  $A-B$  and  $E-F$  bonds after the relaxation in process P-5, one can find that the strain around the dislocation core is biased toward the  $+b$  direction. In the same way, one can also find the dislocation core biased toward the  $-b$  direction after the relaxation in process P-6. The dislocation core is radially symmetric after the relaxation in process P-1. These processes are governed by the effects of the external stress and interaction between dislocations. The initial position of  $r = r_1 \equiv 16.6 \text{ \AA}$  is stable. Because there exists strong external stress after slip of dislocations, the strain field around core is biased toward the direction of slip motion. After unloading the external stress, the strain is biased toward the direction opposite to the previous process, because of the remaining force from the interaction among dislocations.

### 3. Energetics

Let us consider the energetics during the crystal deformation processes. The shear modulus  $\mu$  for Si is already obtained in Sec. IV A as  $\mu = 0.48 \text{ eV}/\text{\AA}^3$ . By using this value,  $K = \mu b^2/2\pi$  is evaluated to be  $1.12 \text{ eV}/\text{\AA}$ . The elastic energy  $E_{elas}^{quad}(r)$  is shown in Fig. 5, calculated from Eq. (A5) in the Appendix. The dislocation-dislocation distance  $r$  in the

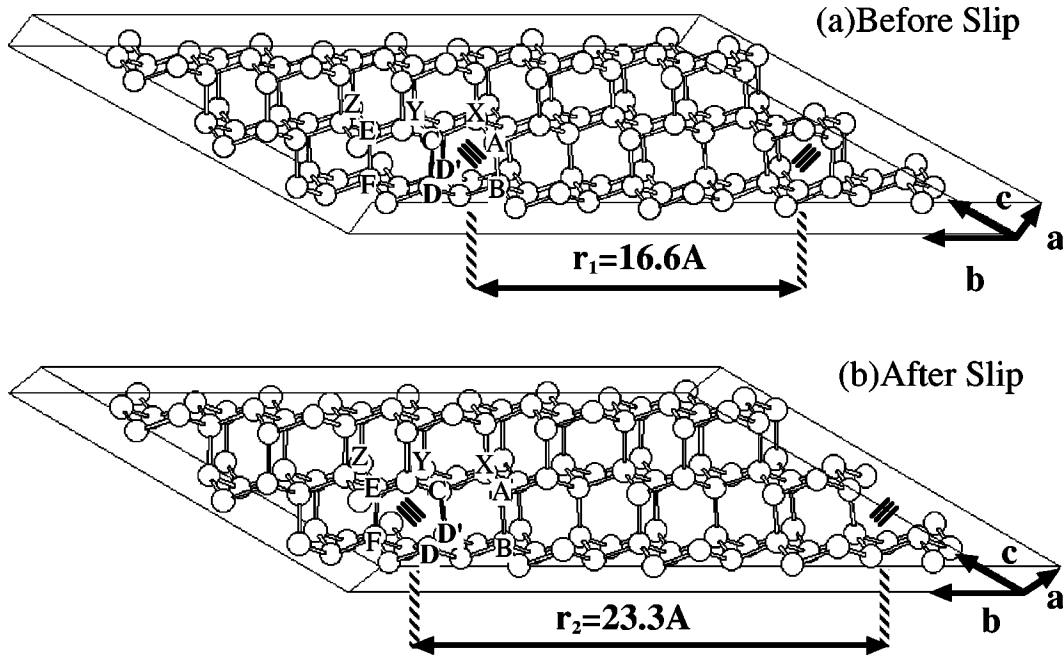


FIG. 4. Atomic configuration in a unit cell observed after the processes P-1 and P-5 of crystal deformation and the structural relaxation. (a) After the P-1 process, which is the initial stable configuration of a dislocation dipole. (b) After the P-5 process (the crystal deformation of  $f_c = 0.4b$ ), which is the final configuration after the dislocation slip.

dislocation dipole is initially set to be  $r = r_1 \equiv 16.6 \text{ \AA}$ . The position of  $r = r_1$  is stable, as is seen in Fig. 5. Therefore, the strain field around the dipole is symmetrical in the relaxed structure of process P-1, as already mentioned. An ideal distance of  $r$  after a slip may be estimated as  $r = r_2 \equiv 23.3 \text{ \AA}$ , which is equal to the value of the initial stable distance plus one translational periodicity of the crystal lattice. In fact, actual shift of the positions of the dislocation core seems to be slightly smaller than that value, due to the fact that the  $r = r_2$  is not a stable position of  $E_{elas}^{quad}(r)$ .

The dislocations slip by only one translational period of the crystal lattice, and stop moving in the present simulation. An isolated dislocation would start to slip when the external stress exceeds the Peierls potential. Once the dislocation starts slipping, it would not stop. In the present simulation, a dislocation moves in the Peierls potential, influenced by the

elastic interactions with other dislocations. From Fig. 5, one can find that the total potential would increase after the slip of one translational period, and the successive slip does not occur spontaneously under the constant external stress. When the external stress increases more, dislocations might restart to slip, and in the end, the dislocation dipole would annihilate.

Assuming a value of the radius of a dislocation core  $r_c = b$  and using  $K = 1.12 \text{ eV/\AA}$ , we can estimate the core energy  $E_{core}$  by Eq. (A4) in the Appendix. The core energy of process P-1 is

$$E_{core} = 0.95 \text{ eV/\AA} \quad (3)$$

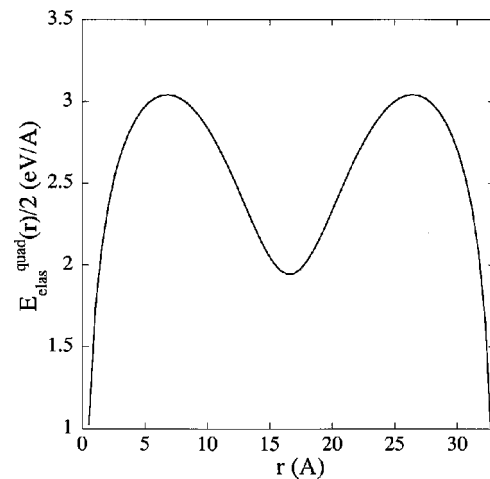


FIG. 5. Half of elastic energy  $E_{elas}^{quad}(r)/2$  as a function of the dislocation-dislocation distance  $r$ .

TABLE I. Changes of bond lengths and angles near the dislocation core after structural relaxation of each process of crystal deformation. Displacement  $f_c$  is shown in parentheses of each process. Values in the parentheses represent the bond lengths of  $C-D'$  and bond angles of  $\angle Y-C-D'$ .

Process ( $f_c$ )	Bond length ( $10^{-2} \text{ \AA}$ )			Bond angle (deg)		
	A-B	C-D	E-F	$\angle X-A-B$	$\angle Y-C-D$	$\angle Z-E-F$
1 (0)	242	242	236	92	127	117
2 (0.1b)	240	245	238	94	130	120
3 (0.2b)	239	248	240	96	135	123
4 (0.3b)	238	256	242	99	140	126
5 (0.4b)	235	382(239)	255	104	147(94)	139
6 (0)	241	342(252)	240	96	147(87)	128

and that of process P-6 is

$$E_{core} = 1.31 \text{ eV/\AA}. \quad (4)$$

These values are not contradict to that from classical MD,<sup>10</sup>

$$E_{core} = 0.72 \text{ eV/\AA}, \quad (5)$$

where the Keating potential<sup>26</sup> and parameters  $r_c = b$  and  $K = 0.69 \text{ eV/\AA}$  are used. If we use just the same value of  $K = 0.69 \text{ eV/\AA}$ , we would estimate at each process as

$$E_{core} = 0.29 \text{ eV/\AA} \quad (\text{the core energy of process P-1}),$$

$$E_{core} = 0.495 \text{ eV/\AA} \quad (\text{the core energy of process P-6}).$$

Because the classical Keating potential reproduces the core structure of an isolated dislocation well, the consistency of  $E_{core}$  between the AIMD and the classical MD means that the superposition assumption is justified.

We discuss the difference of  $E_{core}$  between processes P-1 and P-6. The core energy of a dislocation is independent of the distance relative to other dislocations. And in each process, the crystal is not deformed so that no external stress is loaded. Therefore, the difference of  $E_{core}$ 's between processes P-1 and P-6 originates from the different position of dislocation core relative to the crystal. When the dislocations are well separated, the stable position of dislocation core should be determined by lattice periodicity. In fact, however, the dislocation core in process P-6 is biased towards the  $-b$  direction because of the elastic interactions between dislocations. In other words, the position of the dislocation core has been displaced from the position determined by the lattice periodicity. This means that the dislocations have climbed a certain degree of the slope of the Peierls potential. In the case of process P-1, all dislocations are on the minimum of the Peierls potential because of the configuration of dislocation dipoles. Then the difference of  $E_{core}$  between processes P-1 and P-6 originates from this difference. Much longer systems along the  $[\bar{1}\bar{1}2]$  direction may be necessary to have the same  $E_{core}$ 's of processes P-1 and P-6.

#### 4. Electronic structure

Figure 6 shows the eigenenergies of the one-electron states near the chemical potential as a function of  $f_C$ . The band gap opens when  $0 \leq f_C \leq 0.3b$ . Then it vanishes or the system is metallic at  $f_C = 0.4b$ , i.e., in the atomic configuration after slip of dislocations. After unloading the external stress, band gap opens again or the system is semiconducting again. Based on these results, we can propose the following picture. Just after the slip motion, the bonds near the dislocation core are weakened and the nonbonding state appears when the external stress still remains. So the successive slip would occur much easily than the first slip.

#### 5. Peierls stress from direct method

Let us write an average force due to the external stress on a unit length of straight dislocation  $\vec{F}^{ex}$ . Then  $\vec{F}^{ex}$  is calculated by the Peach-Koehler formula<sup>27</sup> as follows:

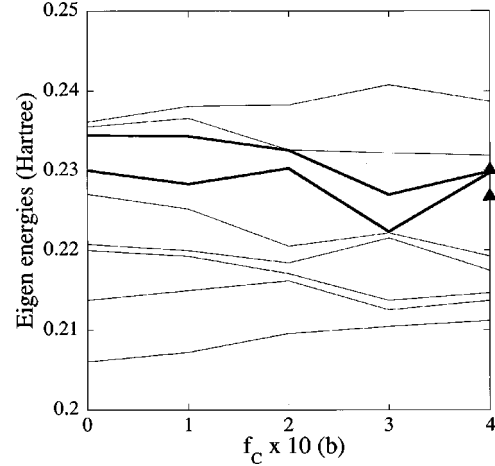


FIG. 6. Eigenenergies near the chemical potential as a function of crystal deformation with the displacement  $f_C$ . The highest occupied and the lowest unoccupied level are shown as bold lines. After process P-6 the gap opens again as denoted by the closed triangles.

$$F_k^{ex} = -\epsilon_{ijk} \xi_i \tau_{jl} b_l, \quad (6)$$

where  $\vec{\xi}$  is a normalized vector parallel to the dislocation line,  $\tau$  is a tensor of external stress,  $\vec{b}$  is Burgers vector, and  $\epsilon_{ijk}$  is a permutation operator defined as

$$\epsilon_{123} = \epsilon_{231} = \epsilon_{312} = 1,$$

$$\epsilon_{132} = \epsilon_{321} = \epsilon_{213} = -1,$$

$$\epsilon_{ijk} = 0 \quad (i=j \text{ or } j=k \text{ or } k=i). \quad (7)$$

These indices of 1, 2, and 3 reveal the directions parallel to the axes of the three-dimensional Cartesian coordinates of the supercell, respectively, and are defined as follows;

- (1) dislocation line  $\vec{\xi}$ , Burgers vector  $\vec{b}$ , i.e.,  $[\bar{1}10]$ ,
- (2) slip direction, i.e.,  $[\bar{1}\bar{1}2]$ ,
- (3) normal vector of slip plane, i.e.,  $[111]$ .

Now the nonzero components of the screw dislocation is only  $b_1$  and  $\xi_1$ , and then only two components  $F_2^{ex}$  and  $F_3^{ex}$  are nonvanishing as

$$F_2^{ex} = \tau_{31} b, \quad (8)$$

$$F_3^{ex} = -\tau_{21} b. \quad (9)$$

The average stress applied on the unit cell was calculated during the simulation. The observed values of  $\tau_{21}$  and  $\tau_{31}$ , evaluated after process P-4 ( $f_C = 0.3b$ ), are

$$\tau_{21} = -0.19 \text{ eV/\AA}^3,$$

$$\tau_{31} = 0.14 \text{ eV/\AA}^3. \quad (10)$$

Generally, a screw dislocation does not have slip plane, so the slip direction is undetermined. In our simulation, the screw dislocation of  $\vec{\xi} \parallel [\bar{1}10]$  in the shuffle set is assumed to

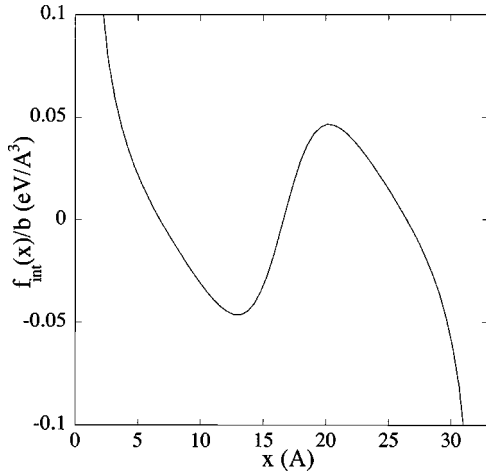


FIG. 7. Stress on a dislocation originated from an elastic interaction energy term among dislocations  $f_{int}(x)/b$ .

be straight, the slip planes can be (111) or  $(11\bar{1})$ . The actual slip was observed to occur on the (111) plane on which the larger stress was applied. Therefore, we can conclude that the external stress causing the dislocation slip is only  $\tau_{31}$  in the present simulation.

Here we will consider how to obtain the Peierls stress from the AIMD simulation. According to the results of our simulation, we should consider the variation of the Peierls potential along to the slip direction parallel to the  $b$  axis. Let us assume a dislocation core is located at the position  $x$  in the  $b$  axis, and we write the Peierls potential at a position  $x$  as  $V_p(x)$ . Since we consider the dynamics of dislocation dipole in a unit cell, a dislocation with an opposite sign moves to a direction opposite each other, and the elastic interaction energy between dislocations  $E_{int}(x)$  changes. The force on a dislocation  $F^{pot}$  is the sum of the forces due to potentials  $E_{int}(x)$  and  $V_p(x)$ :

$$F^{pot}(x) = \frac{d}{dx} V_p(x) + f_{int}(x), \quad (11)$$

where  $f_{int}(x)$  is a force of the elastic interaction  $E_{int}(x)$ . The force  $F^{pot}$  should be equated to the force  $F_2^{ex}$  due to the external stress  $\tau_{31}$ , and then one obtains the following equation:

$$\frac{d}{dx} V_p(x) = -f_{int}(x) + \tau_{31}b. \quad (12)$$

The Peierls stress  $\sigma_p \equiv \max\{(d/dx)V_p(x)\}/b$  can be evaluated by using Eq. (12).

$f_{int}(x)$  is obtained using the same form of the energy calculation as shown in the Appendix. The distance between the dislocation dipole is within the range of  $16.6 \text{ \AA} < r < 23.3 \text{ \AA}$ , so the range of  $f_{int}(x)$  can be estimated from Fig. 7 as

$$0 \text{ eV/\AA}^3 < f_{int}(x)/b < 0.047 \text{ eV/\AA}^3. \quad (13)$$

From Eqs. (10) and (13), one can evaluate the range of value of the Peierls stress without the information of correct evaluation of the position of the dislocation core as

$$0.14 \text{ eV/\AA}^3 < \sigma_p < 0.19 \text{ eV/\AA}^3. \quad (14)$$

We can find that the coincidence between the present estimation and the experimental result  $\sigma_p = 0.043 - 0.215 \text{ eV/\AA}^3$  is excellent. According to the value of  $\sigma_p$ , it is consistent to assume that the screw dislocations in the shuffle set determine the plastic properties of Si at low temperatures.

The PN equation using the GSF energy before structural relaxation produces  $\sigma_p = 0.032 \text{ eV/\AA}^3$ , which is about one order magnitude smaller than the result by the present direct slip dynamics. The plastic properties of the system with small dislocation cores, like semiconductor crystals, are difficult to estimate quantitatively based on the PN theory, as shown in the previous subsection. Now we have demonstrated that the direct method is efficient to estimate the plastic properties quantitatively.

## V. CONCLUSIONS

We have tried two different methods of the simulation for plastic properties of semiconductor materials, i.e., the indirect method based on the GSF energy and the direct method based on the dislocation slip. The direct method gives excellent results of the plastic properties quantitatively.

Our results are summarized as follows:

(1) After structural relaxation, the abrupt bond switching near the dislocation core occurs and this fact implies the narrow core of dislocations, which enhances the applied stress to move dislocations at lower temperatures.

(2) The straight dislocation of shuffle screw is stable. By the crystal deformation towards the  $[\bar{1}10]$  direction, which is parallel to the Burgers vector, dislocation dipoles slip on a (111) plane toward  $[\bar{1}\bar{1}2]$  direction. The slip motion stops after moving by one translational period of the lattice due to the elastic interaction between dislocations in the present configuration of dislocation dipoles. The bonds get weakened around the core structure just after the slip.

(3) By calculating the external stress from first principle, the Peierls stress of the shuffle screw dislocation is evaluated without any artificial modeling of the dislocation core. The Peierls stress obtained for the shuffle plane is consistent with the possibility that slip occurs on this plane.

## ACKNOWLEDGMENTS

We acknowledge Professor K. Maeda and Professor T. Suzuki for useful information and fruitful discussions. The numerical simulations were carried out by the computer facilities at the Institute of Molecular Science at Okazaki, at the Super Computer Center, Kyu-shu University, at the Institute for Solid State Physics, the University of Tokyo, and at the Center for Promotion of Computational Science and Engineering (CCSE) of Japan Atomic Energy Research Institute (JAERI). This work was partially supported by a Grant-in-Aid for COE Research ‘‘Spin-Charge-Photon’’ and

also a Grant-in-Aid from the Japan Ministry of Education, Science, Sport, and Culture.

## APPENDIX

### 1. Energy of dislocations in direct method

The total energy of a system with a dislocation dipole can be written as

$$E_{tot}^{disloc}(r) = E_{tot}^0 + \frac{1}{2} \{E_{cell}^{quad}(r) + E_{int}^{quad}(r)\}, \quad (A1)$$

where  $E_{tot}^0$  is a total energy of deformed perfect crystal with no dislocations,  $E_{cell}^{quad}(r)$  is the self-energy of a dislocation quadrupole, and  $E_{int}^{quad}(r)$  is an elastic interaction energy with the dislocations in the image cells of the dislocation quadrupole. Here, an image cell is a replica of the unit cell generated by a lattice translation.

We will write the projected primitive vectors onto the plane normal to the dislocation line as  $\vec{p}, \vec{q}$ , and define a vector  $\vec{L}_{mn}$  (lattice vector) as

$$\vec{L}_{mn} \equiv m\vec{p} + n\vec{q}, \quad (A2)$$

where the indices  $m, n$  run over all values of integers. The self-energy of a dislocation quadrupole  $E_{cell}^{quad}(r)$  may be written as

$$E_{cell}^{quad}(r) = K \ln \frac{|(-\vec{p} + \vec{q})/2 + \vec{r}| |(\vec{p} + \vec{q})/2 - \vec{r}|}{|(\vec{p} + \vec{q})/2| |(-\vec{p} + \vec{q})/2|} + K \ln \frac{|\vec{r}| |\vec{p} - \vec{r}|}{b^2} + E_{self}^{quad}, \quad (A3)$$

where  $\vec{r} = (r, 0)$ ,  $K = \mu b^2 / 2\pi$ ,  $\mu$  is a shear modulus, and  $r_c$  is a radius of dislocation core. The term  $E_{core}(r_c)$  is the dislocation core energy, which is a constant arbitrarily determined within the approximation of elastic continuum. We will write the constant term of energy as  $E_{self}^{quad}$  by grouping those in Eq. (A3). i.e.,

$$E_{self}^{quad} = K \ln \left( \frac{b}{r_c} \right)^2 + 4E_{core}(r_c). \quad (A4)$$

The elastic interaction energy  $E_{int}^{quad}(r)$  is written as

$$E_{int}^{quad}(r) = \frac{1}{2} K \sum_{m, n \neq 0} \left\{ \ln \frac{|\vec{L}_{mn} + \vec{r}| |\vec{L}_{mn} - \vec{r}|}{|\vec{L}_{mn}|^2} + \ln \frac{|\vec{L}_{mn} + (\vec{p} + \vec{q})/2 - \vec{r}| |\vec{L}_{mn} + (-\vec{p} + \vec{q})/2 + \vec{r}|}{|\vec{L}_{mn} + (\vec{p} + \vec{q})/2| |\vec{L}_{mn} + (-\vec{p} + \vec{q})/2|} + \ln \frac{|\vec{L}_{mn} + \vec{p} - \vec{r}| |\vec{L}_{mn} - \vec{p} + \vec{r}|}{|\vec{L}_{mn}|^2} + \ln \frac{|\vec{L}_{mn} + (\vec{p} - \vec{q})/2 - \vec{r}| |\vec{L}_{mn} - (\vec{p} + \vec{q})/2 + \vec{r}|}{|\vec{L}_{mn} + (\vec{p} - \vec{q})/2| |\vec{L}_{mn} - (\vec{p} + \vec{q})/2|} \right\}, \quad (A5)$$

where the indices  $m, n$  run over all values of integers. Finally, the elastic energy  $E_{elas}^{quad}(r)$  can be written as

$$E_{elas}^{quad}(r) \equiv E_{cell}^{quad}(r) + E_{int}^{quad}(r) - E_{self}^{quad}. \quad (A6)$$

### 2. Interaction forces between dislocations

Suppose that a dislocation is placed on the origin of the two-dimensional Cartesian coordinate, and another dislocation of an opposite sign is placed at  $\vec{x}$  in a unit cell. Then the force acting on the dislocation at  $\vec{x}$  from the dislocation at the origin and other dislocations in the image cells is given as

$$f_{int}(\vec{x}) = K \sum_{m, n \neq 0} \frac{\vec{L}_{mn}}{|\vec{L}_{mn}|^2} + K \sum_{m, n} \left\{ \frac{\vec{L}_{mn} + (\vec{p} + \vec{q})/2}{|\vec{L}_{mn} + (\vec{p} + \vec{q})/2|^2} + \frac{\vec{x} - \vec{L}_{mn}}{|\vec{x} - \vec{L}_{mn}|^2} + \frac{(\vec{p} - \vec{q})/2 - \vec{L}_{mn}}{|(\vec{p} - \vec{q})/2 - \vec{L}_{mn}|^2} + \frac{\vec{L}_{mn} + \vec{x} + (\vec{q} - \vec{p})/2}{|\vec{L}_{mn} + \vec{x} + (\vec{q} - \vec{p})/2|^2} \right\}, \quad (A7)$$

where  $K = \mu b^2 / 2\pi$ . Taking the coordinate parallel to the slip direction,  $\vec{x}$  becomes  $x \equiv |\vec{x}|$ . With the value of  $K = 1.12 \text{ eV}/\text{\AA}$ , the calculated value of  $f_{int}(x)$  is shown in Fig. 7.

- <sup>1</sup>T. Suzuki, T. Nishisako, T. Taru, and T. Yasutomi, *Philos. Mag. A* **77**, 173 (1998).
- <sup>2</sup>T. Yasutomi, T. Tokuoka, I. Yonenaga, and T. Suzuki, *Meeting Abs. PSJ* **53**, 99 (1998).
- <sup>3</sup>T. Suzuki, I. Yonenaga, and H.O.K. Kirchner, *Phys. Rev. Lett.* **75**, 3470 (1995).
- <sup>4</sup>T. Suzuki, *BUTSURI* **53**, 833 (1998).
- <sup>5</sup>J. Castaing, P. Veyssiere, L.P. Kubin, and J. Rabier, *Philos. Mag. A* **44**, 1407 (1981).
- <sup>6</sup>V. Vitek, *Philos. Mag.* **18**, 773 (1968).
- <sup>7</sup>M. Yamaguchi and V. Vitek, *J. Phys. F: Met. Phys.* **3**, 523 (1973).
- <sup>8</sup>E. Kaxiras and M. Duesbery, *Phys. Rev. Lett.* **70**, 3752 (1993).

- <sup>9</sup>J. Hornstra, *J. Phys. Chem. Solids* **5**, 129 (1958).
- <sup>10</sup>T.A. Arias and J.D. Joannopoulos, *Phys. Rev. Lett.* **73**, 680 (1994).
- <sup>11</sup>W. Shockley, *Phys. Rev.* **91**, 228 (1953).
- <sup>12</sup>M. Miyata and T. Fujiwara, *Meeting Abs. PSJ* **53**, 99 (1998).
- <sup>13</sup>M.C. Payne, M.P. Teter, D.C. Allan, T.A. Arias, and J.D. Joannopoulos, *Rev. Mod. Phys.* **64**, 1045 (1992).
- <sup>14</sup>G. Kresse and J. Furthmüller, *Comput. Mater. Sci.* **6**, 15 (1996).
- <sup>15</sup>N. Troullier and J.L. Martins, *Phys. Rev. B* **43**, 1993 (1991).
- <sup>16</sup>L. Kleinman and D.M. Bylander, *Phys. Rev. Lett.* **48**, 1425 (1982).
- <sup>17</sup>J.P. Perdew and A. Zunger, *Phys. Rev. B* **23**, 5048 (1981).
- <sup>18</sup>Y. Juan and E. Kaxiras, *Philos. Mag. A* **74**, 1367 (1996).



- <sup>19</sup>J.R.K. Bigger, D.A. McInnes, A.P. Sutton, M.C. Paynes, I. Stich, R.D. King-Smith, D.M. Bird, and L.J. Clarke, *Phys. Rev. Lett.* **69**, 2224 (1992).
- <sup>20</sup>H.J. McSkimin, *J. Appl. Phys.* **24**, 988 (1953); H.J. McSkimin and P. Andreatch, Jr., *ibid.* **35**, 3312 (1964).
- <sup>21</sup>J.R. Rice, *J. Mech. Phys. Solids* **40**, 239 (1992).
- <sup>22</sup>B. Joós, Q. Ren, and M.S. Duesbery, *Phys. Rev. B* **50**, 5890 (1994).
- <sup>23</sup>T. Suzuki and S. Takeuchi, *Lattice Defects in Ceramics*, edited by S. Takeuchi and T. Suzuki (Publ. Off. of Jpn. J. Appl. Phys., JJAP Series No. 2, Tokyo, 1989), p. 9.
- <sup>24</sup>C.W. Garland and K.C. Park, *J. Appl. Phys.* **33**, 759 (1962).
- <sup>25</sup>W. Harrison, *Electronic Structure and the Properties of Solids* (W.H. Freeman, San Francisco, 1980).
- <sup>26</sup>P.N. Keating, *Phys. Rev.* **145**, 637 (1966).
- <sup>27</sup>J.P. Hirth and J. Lothe, *Theory of Dislocations*, 2nd ed. (Wiley, New York, 1982).